

Journal of Biomedical Optics

BiomedicalOptics.SPIEDigitalLibrary.org

Overview of single-cell elastic light scattering techniques

Matti Kinnunen
Artashes Karmenyan

Overview of single-cell elastic light scattering techniques

Matti Kinnunen^{a,*} and Artashes Karmenyan^{b,c}

^aUniversity of Oulu, Optoelectronics and Measurement Techniques Laboratory, P.O. Box 4500, 90014 Oulu, Finland

^bNational Yang-Ming University, Biophotonics and Molecular Imaging Research Center (BMIRC), Taipei 11221, Taiwan

^cNational Dong-Hwa University, Department of Physics, Hualien 97401, Taiwan

Abstract. We present and discuss several modern optical methods based on elastic light scattering (ELS), along with their technical features and applications in biomedicine and life sciences. In particular, we review some ELS experiments at the single-cell level and explore new directions of applications. Due to recent developments in experimental systems (as shown in the literature), ELS lends itself to useful applications in the life sciences. Of the developed methods, we cover elastic scattering spectroscopy, optical tweezer-assisted measurement, goniometers, Fourier transform light scattering (FTLS), and microscopic methods. FTLS significantly extends the potential analysis of single cells by allowing monitoring of dynamical changes at the single-cell level. The main aim of our review is to demonstrate developments in the experimental investigation of ELS in single cells including issues related to theoretical “representations” and modeling of biological systems (cells, cellular systems, tissues, and so on). Goniometric measurements of ELS from optically trapped single cells are shown and the importance of the experimental verification of theoretical models of ELS in the context of biomedical applications is discussed. © The Authors. Published by SPIE under a Creative Commons Attribution 3.0 Unported License. Distribution or reproduction of this work in whole or in part requires full attribution of the original publication, including its DOI. [DOI: [10.1117/1.JBO.20.5.051040](https://doi.org/10.1117/1.JBO.20.5.051040)]

Keywords: elastic light scattering; elastic scattering spectroscopy; single cell; goniometer; optical tweezers; microscopy; Fourier transform light scattering; flow cytometry.

Paper 140678VRR received Oct. 15, 2014; accepted for publication Feb. 13, 2015; published online Mar. 11, 2015.

1 Introduction

New optical methods in biomedical research, providing a wide range of information concerning the studied biological object, include optical coherence tomography,^{1–3} surface-enhanced Raman scattering,^{4,5} surface plasmon resonance,^{6–8} and coherent anti-Stokes Raman scattering spectroscopy.⁹ Yet another widely used method is elastic light scattering (ELS) from cells and tissues.

ELS patterns depend on many factors such as the size and shape of the object, relative refractive index between the object and the surrounding medium, as well as the wavelength of light. To understand the behavior and connections behind light scattering from particles and measured light scattering distributions, several theoretical approaches have been advanced. They have highlighted the ratio between the size of the object and the used wavelength. Although geometric approximation and Rayleigh scattering regimes can be easily distinguished, the number of objects falling outside the scope of these theories makes quantitative analysis challenging. Particularly in the intermediate range, where particle size and wavelength are comparable, light scattering by spherical objects can be described by Mie theory.¹⁰ Moreover, different computational methods have been developed for a theoretical analysis of light scattering in that range.^{11–14} Continuous progress is being made in theoretical research in this field: Theoretical reviews are published, computational and simulation problems are elucidated,^{15,16} and a database of theoretical work is updated periodically.^{17,18}

After the introduction of the light scattering method, much research work has been devoted to determining the size of spherical particles and measuring the angular light scattering of aerosols.^{19,20} Other applications include mineral and soot aerosols, volcanic ashes, snow and ice crystals, dust, and a range of particles of different shapes in astrophysical environments.²¹ Also single-cell applications and analysis have attracted a lot of attention. Because intracellular structures have a refractive index distribution and they affect light scattering, extensive work has been conducted to understand the origin of ELS in the identification of cells, to analyze intracellular structures, and to develop models for light scattering from cells.^{22–24} Forward-scattered light is primarily dependent on the size and refractive index of the cell under study,²⁵ as well as its shape and morphology,²⁵ whereas scattering at larger angles (50 deg to 130 deg) depends on the cell’s internal structure.^{26–28} Typically, the diameter of a mammalian cell is 10 to 30 μm , while the diameter of the nucleus is in the range of 3 to 10 μm .²⁹ Several attempts have been made to measure the full-phase function in biological cells^{30–33} in order to provide a basis for detailed characterization. ELS also forms the foundation for commercial flow cytometry systems, measuring light scattering at different angles.^{34,35} ELS can be used to characterize biological thin samples and to differentiate the origin of sub-cellular structures.^{36,37} ELS can also be utilized to calculate the anisotropy parameter of cells, cell suspensions, and tissues, which provides valuable information for developing different types of optical noninvasive methods of investigation and can also be used to confirm theoretical predictions.^{24,38} ELS can be used to study the connection between cell structure and light scattering patterns, which is very important for optical

*Address all correspondence to: Matti Kinnunen, E-mail: matti.kinnunen@ee.oulu.fi

diagnostic methods.^{28,36,38,39} In addition, instead of measuring angular distribution, elastic scattering spectroscopy (ESS) enables characterizing the sizes of subcellular components from backscattering measurements of cells and tissues.^{37,39-41}

Many directions of research based on light scattering can be considered as ELS. A range of such methods has been presented and widely discussed in reviews and books (e.g., see Refs. 10, 36, 38, 39, and 42). Additionally, new interesting directions and specific methods are being developed, some of which have yet to appear in review papers. The development of new directions and methods often combines with the development of new technologies and the improvement of present techniques and devices with new modern approaches to known problems. This paper points out some of these new methods and approaches in order to draw researchers' attention to them. In this way, they may serve as an initial impetus for other researchers.

In addition to covering basic concepts, we shall focus on explaining and discussing different measurement principles and methods of analysis that can be used to measure ELS from single cells and subcellular structures. We are keen to present the application of ELS to single-cell scattering and to present available software for ELS analysis and modeling. This paper demonstrates some approaches to ELS applications including ESS, optical tweezers in combination with a goniometer, flow cytometry (based on ELS), and light-scattering measurement principles such as Fourier transform light scattering (FTLS), in conjunction with a microscope. Recent results of the authors will also be discussed, and examples of published data will be shown. Overall, this review aims to provide a comprehensive and easily accessible resource on ELS in a narrow and little noted application domain.

2 Theoretical Aspects

ELS studies were begun in the second half of the 19th century,⁴³⁻⁴⁵ and the scattering problem was theoretically described at the beginning of the 20th century.⁴⁶⁻⁴⁸ Extensive literature already exists on the history and theory of ELS from single particles.⁴⁹⁻⁵⁶ Due to new methods and current technical progress in computation, ELS methods are being developed in a number of directions, and new applications are constantly being found and investigated. Together with research papers, review papers and books are being published on some rapidly developing application areas of elastic scattering^{10,38,39,42} including flow cytometry⁵⁷⁻⁶⁰ and light scattering spectroscopy.⁶¹

Theoretical background and analysis of methods related to ELS in the biomedical context, particularly at the single-cell level, are described in some books.^{36,61} Cell behavior in different conditions, including interaction with nanoparticles, has been described and new models have been developed for various shapes of cells with an internal structure.⁵⁹ These models include finite-difference time-domain (FDTD) modeling of clusters of nanoparticles in cell cytoplasm or randomly distributed nanoparticles on the surface of the cell nucleus,⁵⁹ mononuclear cells with an inhomogeneous core,⁵⁹ and a neutrophil model with nucleus.⁶² In addition, light scattering from cells and isolated nuclei has been modeled and measured.⁶³ Models have also been presented for multicellular spheroids and their scattering has been compared with that of single cells.⁶⁴ At the single-cell level, ELS measurements must fulfill certain conditions for single scattering. They are: (1) multiple scattering can be assumed to be negligible, (2) the scatterer will only be exposed to radiation from the original laser beam, and (3) light scattering

from the particle will not be subjected to further scatter by another particle.³⁶ In the single particle case, the incident plane wave will hit the particle and scatter as a spherical wave. When illuminating a particle or cell with a plane wave, the relation between the incident and scattered fields will be given by Eq. (1)³⁶ (see also Refs. 49, 51, and 65):

$$\begin{pmatrix} E_{ls} \\ E_{rs} \end{pmatrix} = \begin{pmatrix} S_2 & S_3 \\ S_4 & S_1 \end{pmatrix} \cdot \frac{e^{-ikr+ikz}}{ikr} \begin{pmatrix} E_{li} \\ E_{ri} \end{pmatrix}, \quad (1)$$

where S_{1-4} are the complex functions of θ and ϕ with amplitude and phase and can be represented in a matrix form:

$$S = \begin{pmatrix} S_2(\theta, \phi) & S_3(\theta, \phi) \\ S_4(\theta, \phi) & S_1(\theta, \phi) \end{pmatrix}.$$

E_i is the incident field, whereas E_s is related to the scattered field. The letters l and r denote parallel and perpendicular polarizations of the E field, respectively. θ is the angle between the incident and scattered directions, whereas ϕ denotes the azimuthal angle of scatter. Information on light scattering from a single scatterer can be obtained by a calculation of the elements in a Müller matrix $[S]$.^{36,66} This matrix provides information on cell morphology,⁶⁶ but it can also reveal details about the polarization of light propagating in a multiple scattering medium.⁶⁷ Because an analytical solution of the problem is challenging and has been calculated for spheres,^{49,50} numerical approaches have been developed for ELS from arbitrarily shaped particles. At the moment, the T-matrix^{11,12} and FDTD¹³ methods, developed by Waterman and Yee, respectively, are commonly used to model light scattering from single cells and cell organelles (e.g., Ref. 24). Much progress in this field has also been made by faster and more advanced calculation methods.⁶⁸⁻⁷³ References related to T-matrix calculations are systematically updated in a T-matrix database of references, making it the most commonly used method for ELS calculations today.^{17,18}

ELS distribution is affected by several factors such as polarization of light, refractive index (n), particle size and shape, and the wavelength of the light. The size parameter α defines the ratio between particle size and wavelength:

$$\alpha = \frac{\pi d}{\lambda}, \quad (2)$$

where d is the particle diameter and λ is the wavelength. This relation is important in ESS.^{40,74} Other important factors for describing light scattering at the single particle and cell level are the relative refractive index $m \equiv n_s/n_0$ (n_s is the refractive index of the scatterer, and n_0 is the refractive index of the surrounding medium) and the scattering cross-section. The scattering cross-section per particle can be presented as Eq. (3),^{65,75} which is suitable for experimental evaluations:

$$\sigma_{\text{sca}} = (\lambda^2/2\pi)(1/I_0) \int_0^\pi I(\theta) \sin \theta d\theta, \quad (3)$$

where I_0 is the intensity of the incident light, $I(\theta)$ is the angular distribution of the intensity of light scattered by the particle, and θ is the scattering angle. However, it is worth remembering that Eq. (3) assumes the particles to be spherical. For a dielectric sphere (Mie theory) with parameters close to a red blood cell (RBC) irradiated by visible or NIR light ($g > 0.9$,

$5 < \pi d/\lambda < 50$, $1 < m < 1.1$), the scattering cross-section can be approximated as⁷⁶

$$\sigma_{\text{sca}} \sim [3.28\alpha^{0.37}](m-1)^{2.09}/(1-g), \quad (4)$$

where α represents the size parameters [Eq. (2)], $m \equiv n_s/n_0$ is the relative refractive index of the particle, and g is the scattering anisotropy factor, defined as the mean cosine of the scattering angle θ ,³⁸

$$g \equiv \langle \cos \theta \rangle = \int_0^\pi p(\theta) \cos \theta \cdot 2\pi \sin \theta d\theta, \quad (5)$$

where $p(\theta)$ is the phase function that describes the scattering properties of the particle and is the probability density function for scattering in some direction of a photon travelling in another direction. $p(\theta)$ is a nondimensional phase function, whose integral over the solid angle is equal to 1.^{49,50} ELS measurements, conducted in cell suspensions and at the single-cell level, enable an estimation of the anisotropy parameter g . It is an important parameter, describing the directivity of a scattering event and is used as an input parameter when simulating light propagation in tissues and cells.^{38,77} It has also been shown that the light transport depends on the exact form of the angular scattering probability distribution.⁷⁸

The Internet offers a variety of programs for calculating the characteristics of ELS particles (cells) with different parameters. A number of these programs are available on special sites,^{79–87} which offer the possibility to calculate ELS and other relevant parameters such as scattering, absorption, and attenuation cross-section,⁸¹ from homogeneous spheres,⁷⁹ coated spheres,⁸¹ and multilayer spheres.⁸⁰ Some papers describe the possibility of direct online simulation, calculation, and analysis.^{15,16,85–87} This is a highly welcome development as it saves valuable research time for scientifically interesting problems. Software at different levels of sophistication is provided for free use.^{87–90}

3 Available Techniques

Several techniques have been developed to detect ELS from cells and tissues. In this paper, we describe some methods enabling the measurement of ELS at the single-cell level. One commonly utilized device in ELS is the goniometer, which has been used in a wide range of applications to measure ELS in diluted cell concentrations,^{91,92} cell suspensions,^{28,37,93,94} and single cells^{33,95} using either a cylindrical cuvette, as in Fig. 1, or a slab cuvette. Other methods combine scattering light intensity detection methods with a microscope, which also enables measuring dynamic light scattering (DLS) from cells. These techniques include FTLS, which allows simultaneous measurement of ELS and DLS properties.⁹⁶ This approach lends itself to monitoring changes in cell membrane dynamics.

3.1 Elastic Scattering Spectroscopy

ESS measures backscattered light from a sample illuminated by a white light source (e.g., xenon arc lamp⁴⁰). Relative scattering intensity, $I_s(\lambda)/I_0(\lambda)$, is measured at a known scattering angle. Strongly dependent on the size parameter, relative scattering intensity is a linear combination of the spectra of different sub-cellular components.⁴⁰ Relative intensity is sensitive to particle size⁹⁷ and ESS provides information about the size of sub-cellular structures.^{41,97,98} A lot of effort has gone into trying to understand the theoretical basis of these phenomena and to

experimentally confirm theoretical results.^{40,74,99} A recent application involves monitoring apoptosis on the basis of morphological changes in cell cultures.^{41,98}

3.2 Detection of Angular Dependence of Scattering

A typical goniometric setup for the ELS measurement of single cells and cell suspensions consists of a light source, cuvette, detector, and rotating arm (Fig. 1). A stepper motor is used to rotate the detector around the sample at specific steps. These setups typically use an HeNe laser as a light source.^{28,33,100,101} Other approaches include multiple lasers at different wavelengths,⁶⁶ a short arc Xe lamp with interference filters,¹⁰² a laser diode,¹⁰³ or a coherent white-light supercontinuum laser.¹⁰⁴

When using a phase-sensitive detection method, a chopper is implemented between the laser and the cuvette to modulate the beam.¹⁰¹ Cleaning and limiting beam size may also require the use of additional focusing optics and apertures.^{99,103} Moreover, neutral density filters are used to extend the dynamic range of the system, because the detector's dynamic range is limited and forward-scattered light tends to be very strong.^{28,33}

On the detection side, a typical setup includes mechanical apertures to limit the field-of-view, an optical lens to collect scattered photons, and a sensitive detecting element attached to a motorized rotating stage.^{28,33,100} Various detectors have been used in ELS measurements (different cuvettes and configurations). Brunsting and Mullaney¹⁰⁵ measured light scattering with a photometer using a high-speed film as the detector, Arnfield et al. used a radiometer,¹⁰⁶ and several other researchers have relied on photodiodes.^{92,93,107} Doornbos et al.³³ used an avalanche photodiode. When the field-of-view is limited by a pinhole, it is also possible to use a power meter.⁹¹ Also photomultiplier tubes (PMTs) have been commonly used in recent studies (e.g., see Refs. 28, 100, and 108–111).

In typically used cylindrical cuvettes (see Fig. 1), a detector rotates around the sample and measures light scattered from it.¹⁰¹ Scattering that originates from the background suspension can be decreased by reducing the path length of light in the suspension, for example, by using a smaller cuvette. When measuring ELS from a single object, special attention must be paid to sample purity and filtering of all unwanted dust and particles from the background medium.^{33,100}

It is typical for goniometric measurements to take several minutes or even several tens of minutes. As a result of the long measurement time for each scattering angle, time-dependent information can easily be averaged.³³ To reduce the measurement time, Watson et al.⁹⁵ developed a system that employs an elliptical reflector instead of a stepper-motor rotation stage. In this setup, a fast rotating aperture disk (up to 2000 revolutions per minute) was used in front of the detector to specify the receiving angle at a specific time. This enables measuring ELS from trapped cells with high temporal resolution (in the

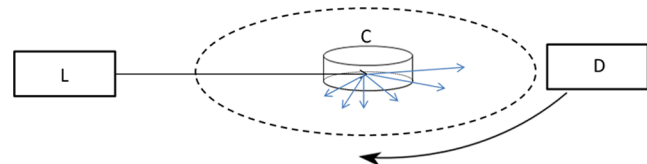


Fig. 1 Basic components of a typical goniometric setup with a cylindrical cuvette. L—light source, C—cuvette, and D—detector/detection optics.

range of a few tens of milliseconds). Also optical fibers can be used to receive light at different angles and to guide light into the detector. Wyatt,¹¹² as well as Holthoff et al.,¹⁰⁸ describe a multi-angle measurement system using several optical fibers simultaneously. Foschum and Kienle¹⁰³ measured ELS with a detector in a fixed place. These setup configurations can potentially be used in conjunction with an optical trap to select a single particle or cell for measurements.

Nephelometry is a method to measure scattering phase functions of particles in a suspension. Originally, the method was developed to measure scattering phase functions of aerosol particles using an elliptical reflector.¹¹³ Thereafter, a setup using off-axis parabolas, a mirror on a motorized stage, and confocal imaging was developed to measure the angular light scattering from particle suspensions and to define the size of the particles.^{114,115}

Other possible instrumentation approaches to measure ELS from cells include slab cuvettes with different thicknesses for cells, tissues, and tissue phantoms.^{37,91,92} In most cases, sample thickness is reduced and cell samples are diluted to reach the single-scattering regime.^{91,92} The shape of the cuvette may limit the scattering angles detectable by the instrument. Additional computing may be necessary to interpret the results.⁹² A novel technique, using a white light source, enables a new type of multiwavelength investigation of single particles and cells, and the principle was recently demonstrated using a slab cuvette and reflection-mode configuration.¹⁰⁴ This instrument enables measuring hyperspectral, polarimetric, and angular light-scattering and was used to measure the properties of an *in vitro* model, namely multicellular tumor spheroids.

3.3 Optical Tweezer-Assisted Elastic Light Scattering Studies

Optical tweezers offer a noncontact method for capturing single particles and cells in a trap.¹¹⁶ They enable interaction force measurements and manipulation of micro-objects. Wright et al.¹¹⁷ demonstrated the usage of infrared optical tweezers for trapping a single cell in a microscope and measuring the diffraction profiles of a trapping laser diffracted from the cell by using a photodiode array. Optical tweezers can keep a particle or a cell in one place [Fig. 2(a)], while scattering patterns are measured around it by a goniometric detector in a plane orthogonal to the trapping beam [Fig. 2(b)].^{33,95,100} It is worth noting that the orthogonal measurements allow viewing an image of the scattering distribution around a trapped cell on a video camera (from the bottom or top direction of the cuvette).^{95,100} This image can be used as an aid to system adjustment as well as for analytic

purposes to determine fast, dynamic changes in light scattering (see Fig. 4). Optical tweezers come in a variety of constructions. They can be formed using a high numerical-aperture water-immersion objective (NA = 1.0),¹⁰⁰ two counter-propagating beams with low numerical-aperture objectives (NA = 0.4),³³ or in an inverted microscope using a low numerical-aperture lens (NA = 0.68).⁹⁵ When the trapping laser and light-scattering measurement laser (HeNe) are orthogonal to each other, long working-distance objectives must be used to trap particles to prevent them from affecting and distorting the wave shape of the HeNe laser. Another important consideration is that the cells must be lifted far up from the bottom of the cuvette to minimize reflections from it.^{100,109}

It is possible to use several traps to fix the position and orientation of the cell under study.^{100,111} Further, cylindrical lenses can be used to modify the intensity distribution of trapping lasers, which allows trapping several cells during ELS measurements.¹⁰⁹ Special attention must be paid to the stability of the traps, the power of the trapping laser, possible heating of the sample, and potential cell damage. In most cases, an IR laser with a moderate trapping power (a few tens of milliwatts) is suitable for this type of experiment.

More recently, supercontinuum white light has been used to trap and characterize a single particle.¹¹⁸ The researchers behind this feat also studied optical scattering spectroscopy of a single spherical scatterer, illuminated with a tightly focused supercontinuum light.¹¹⁹ A wide spectrum of different wavelengths enables droplet size determination by observing the spectrum of the on-axis backscattered light. In contrast to monochromatic trapping, the broad spectrum of supercontinuum light covers several resonances of the first excited Mie coefficients.¹²⁰

ELS distributions depend on the size of scattering structures.^{121,122} Thus, to develop characterization, it is important to measure ELS in a wide angular range. As different cells have been characterized by flow cytometry and in cell suspensions, single-cell measurements with optical tweezer-assisted systems offer the advantage of more detailed analysis. Doornbos et al.³³ measured ELS of a lymphocyte in the angular range of 20 deg to 60 deg. However, they experienced problems with cell stability in the trap during the measurements. Watson et al. conducted more detailed measurements on ELS and the behavior and dynamic changes of trapped cells. Figure 3 shows the measured scattering diagram from a lymphocyte and a granulocyte in a wide angular range. As seen, ELS has the ability to reveal differences between cells. An experimentally determined phase function contains information obtained from different particles in cells and can identify morphological

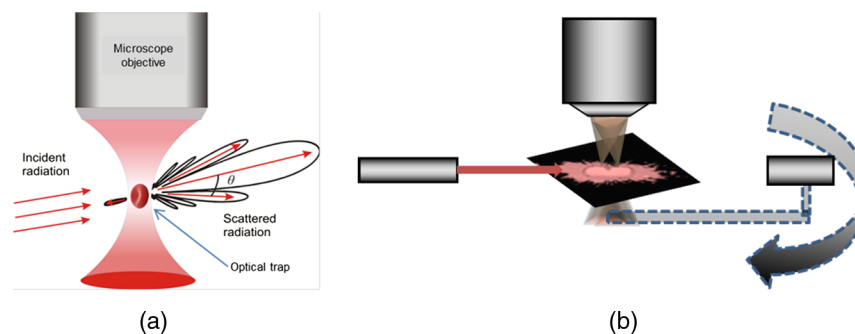


Fig. 2 Schematic of an optically trapped red blood cell (RBC) (a) (modified from Ref. 110) and a combination of a double-beam optical trap and goniometric setup (b).

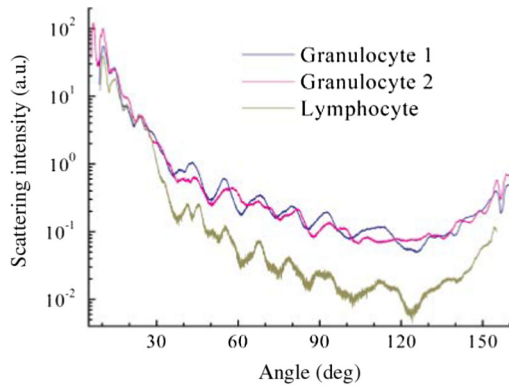


Fig. 3 Light-scattering diagrams of a normal blood lymphocyte (lower curve) and two different granulocytes (two upper curves). [Reprinted from Ref. 95, Copyright (2004), with permission from Elsevier.]

differences. Detailed information about cells can be used for sensitive label-free analysis and cell sorting. Their group studied the effect of cell motility and rotation in the trap and found that the trapped cells oscillate a little on the millisecond time scale.⁹⁵

Although optical tweezers offer a clear advantage in terms of separating single cells, there are also some problems associated with scattering measurements involving a cell in an optical trap. In single-cell measurements, possible problems with optical tweezers include cells sticking to the glass cuvette, changes in cell orientation (scattering intensity fluctuations), and convection flows.^{33,95,100} Sticking can be overcome by coating the cuvette with an appropriate material (pluronic³³ and agarose⁹⁵), while changes in cell orientation and convection flows can be overcome by decreasing the size of the cuvette and increasing the power of the trap. Double-beam optical tweezers enable controlling and fixing RBC orientation during ELS measurements [Figs. 2(b) and 4].^{100,109}

As isovolumetric sphering of RBCs is typically used in flow cytometry measurements,¹²³ by which the theoretical models of single cells can be easily compared with those of homogeneous spheres. Also spherical models with coatings have been developed to mimic light scattering from cells and to analyze light scattering.^{23,124} However, they do a fairly poor job of representing real RBCs. Several theoretical attempts have been made to model ELS in RBCs, including a spheroid model,^{68–70,125–129} and they show that the scattering is affected by the thickness, orientation, and shape of the cell under study.^{126,127} Figure 4 also shows that the shape of the RBC affects light scattering. Therefore, it is important to analyze differences in the scattering patterns of spheres or spherical RBCs. These differences were experimentally demonstrated in our previous work.¹⁰⁰ Theoretical models for ELS from RBCs based on equivalent sphere or oblate spheroid approximations are not optimal.¹²⁵ The latter type, for example, is only applicable to face-on incidence in a limited angular range (0 deg to 4 deg).

Essentially, the ELS technique is based on the assumption that a single-scattering regime exists in the sample and involves calculating the size and refractive index of single particles and cells. When two cells are too close to each other, dependent scattering may occur. As a result, scattering from different particles is no longer independent, as the distance and orientation of the cells in relation to the incoming laser beam induce the interference in the scattered and incoming beams. Figure 4 shows that the optical tweezers with point and elliptical traps enable adjusting the number and orientation of RBCs in measurements.¹⁰⁹

Our previous work¹¹¹ showed that two-point traps allow us to adjust the place of polystyrene spheres and RBCs and to measure dependent scattering between real cells in a phosphate-buffered saline (PBS). Thus, it is now possible to investigate dependent scattering problems experimentally, which was earlier possible only in theory.^{126,128}

Modeling light scattering from multiple RBCs is more complicated than modeling based on single cells, since multiple scattering effects need to be considered. Results by He et al. show that, although the lateral distance of cells in face-on orientation may change, scattering probability distributions remain almost unaffected. Simulations with several cells in face-on orientation along the direction of the incident beam showed that multiple scattering becomes more pronounced and can no longer be neglected.¹²⁸

3.4 Fourier Transform Light Scattering

The FTLS method can be incorporated into a computer-controlled microscope to detect ELS. A general requirement for this method is accurate phase retrieval of the scattered field, which can be accomplished with a common path interferometer. Moreover, the illumination light beam must have full spatial coherence.^{96,130} Far-field scattering patterns are calculated from electric field measurements using a two-dimensional (2-D) Fourier transform.^{131,132} Capable of measuring both ELS and DLS, the FTLS method offers a powerful tool for characterizing biological cells. FTLS can reveal fine details in the ELS signal obtained from different cells. Ding et al.⁹⁶ demonstrated that this method is capable of differentiating between several cell types including RBCs, myoblasts (C2C12), and neurons. Further, Park et al. have shown that FTLS can be used to identify and distinguish intraerythrocytic stages of *Plasmodium falciparum* malaria (Fig. 5). In addition, FTLS can show differences in normal and ATP-depleted RBCs and reveal correlations between ATP levels and the mechanical properties of RBCs,¹³¹ as well as measuring the Hb-content of single cells using the spectroscopic approach.¹³² In order to enhance the benefits of the FTLS method, single cell studies can be extended to cover blood smears. Lim et al. have developed faster analysis of ELS signals with FTLS method. A Born approximation allows calculating several parameters including the diameter and thickness as well as the depth and width of the dimple region from blood smears, enabling high-throughput analysis.¹³³ FTLS method can also reveal changes in the shape of the object under study by measuring the anisotropic nature of the scattering signal. A case in point is the ELS distribution of normal and sickle cells.¹³⁴ Recent developments of this technique include demonstrating light scattering measurements and characterizing single rod-shaped bacteria, which open new application perspectives for applications such as microfluidic sorting.¹³⁵

Using a white light source allows measuring the spectroscopic angular scattering properties of microscopic objects. Jung et al. demonstrated the usage of swept-source FTLS with polystyrene spheres. This method lends itself to investigating diseases such as malaria and sickle cell anemia.¹³⁶

3.5 Microscopic Methods

Due to the standardized sample preparation protocols and sample holders, microscopic instruments and their modifications have obtained increasing interest. Brock et al.¹³⁷ used confocal imaging and automated image processing to reconstruct

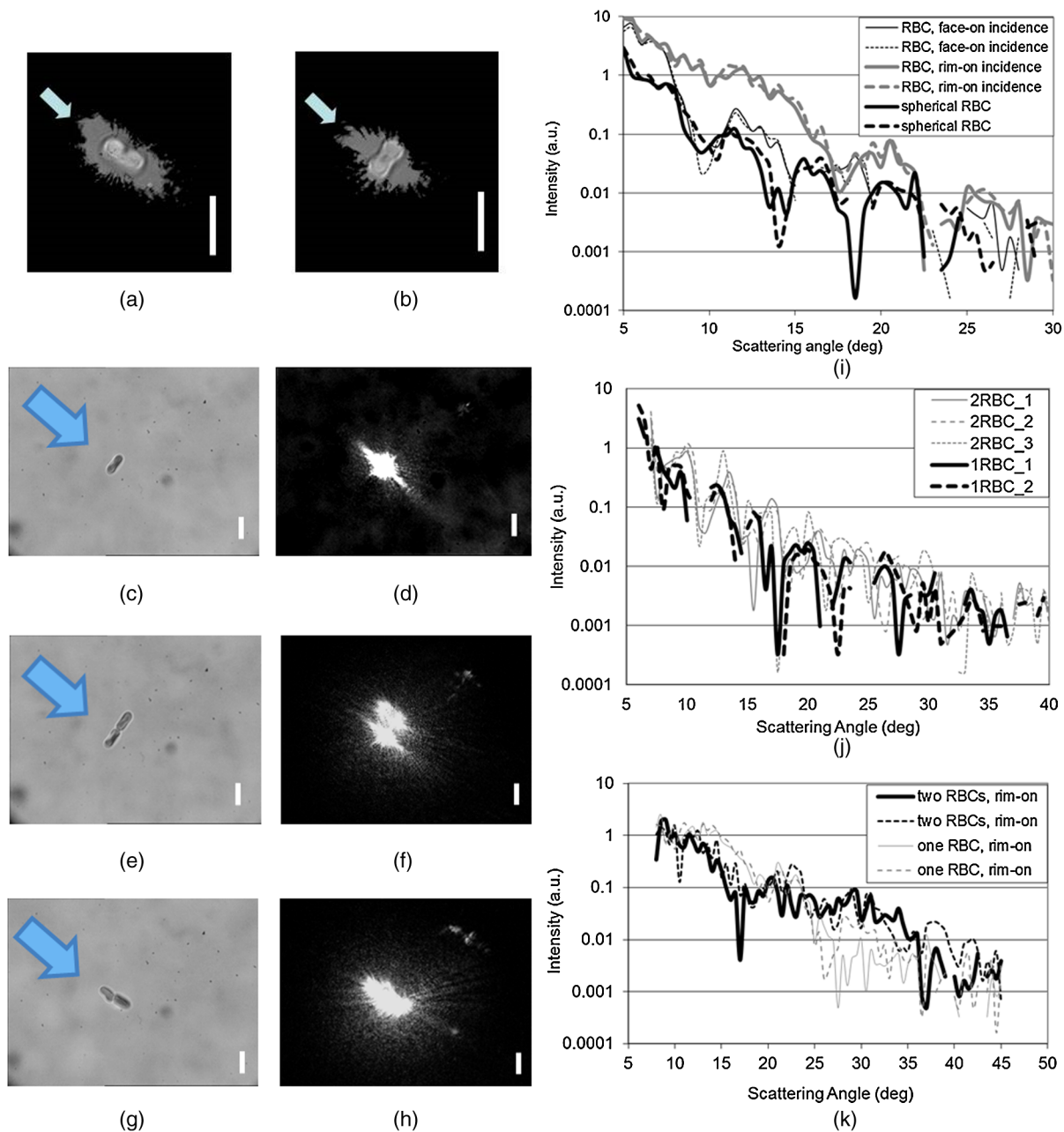


Fig. 4 Trapped RBCs in different orientations, light scattering image in the orthogonal direction, and corresponding ELS distribution. Face-on incidence: (b), (c), and (e) and rim-on incidence: (a) and (g). (i) shows the scattering distributions from cells in (a) and (b), (j) scattering distributions from cells in (c) and (e), and (k) scattering distribution from cells in (g). (d), (f), and (h) show the camera images of light scattering distributions from trapped cells in (c), (e), and (g), respectively, when sample lighting has been turned off and the HeNe laser has been turned on. The arrow shows the direction of the incident laser light. (Modified from Refs. 100 and 109.)

a three-dimensional (3-D) model of NALM-6 cells from a stack of 2-D images. Further, they used the FDTD method to calculate angle-resolved light-scattering distributions and Müller matrix elements for the reconstructed 3-D cell and compared the ELS distributions of the reconstructed cells with those of homogeneous and coated-sphere models. They showed that the coated-sphere model is appropriate for B-cells only in the forward direction (0 deg to 20 deg), and that this region can be used to estimate the phase function. At higher angles, however, the coated-sphere model proved useless.¹³⁷

As an extension of typical confocal microscopy, Itzkan et al.¹³⁸ developed a confocal light absorption and scattering spectroscopic microscope which combines a confocal microscope with light-scattering spectroscopy. This microscope allows measuring the size, shape, refractive index, and location of particles smaller than the diffraction limit without exogenous labeling. Hence, it is suitable for observing submicrometer intracellular structures within living cells.¹³⁸

More recently, Richter et al.¹³⁹ demonstrated measurement of backscattered angular light distributions from cells using an

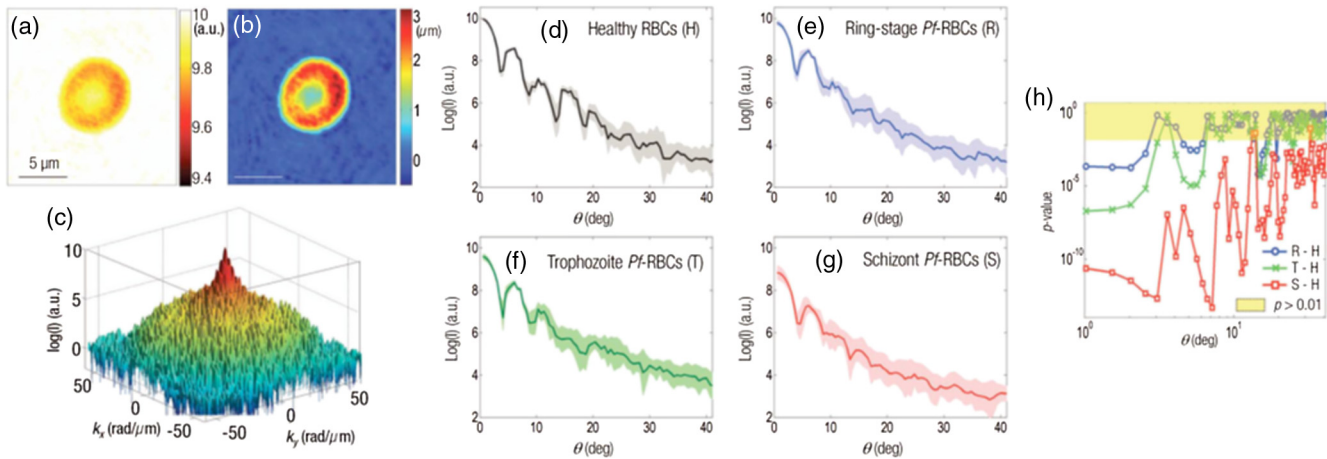


Fig. 5 (a) Amplitude and (b) phase map of a healthy RBC. (c) A retrieved light scattering pattern of the same cell. Light-intensity scattering patterns of (d) healthy RBCs, (e) ring, (f) trophozoite, and (g) schizont stages of Pf-RBCs. (h) p -Values of scattering patterns of different intraerythrocytic stages of Pf-RBCs are compared with healthy RBCs. (Reprinted with permission from Ref. 131.)

inverted microscope and additional laser light illumination. A laser diode at the wavelength of 470 nm was used on the illumination side, while the detector was a PMT. They used ELS for cell differentiation before and after apoptosis, which induces shrinking of cells and alteration of cell shape. Richter et al. found an increase in backscattered light as a function of time in response to apoptosis induced by staurosporine. Light scattering was found to be a good complementary tool to microscopic imaging for label-free detection of apoptosis and may represent a first step toward label-free *in vivo* diagnostics.¹³⁹

3.6 Flow Cytometry

Flow cytometry with different modifications is a well-known technique for light scattering-based cell characterization and has been reviewed in a number of books and review publications.^{57–60} It has the capacity to identify cells with high flow rates, and the analysis is based on determining their size and refractive index from the recorded scattering distributions. It also allows presenting the achieved results in cytograms and histograms.¹⁴⁰ Flow cytometers use, among others, laser diodes and several detectors fixed at different angles to determine the strength of the light-scattering signals,^{140,141} whereas scattering flow cytometry enables the measurement of ELS in a wider angular range.^{34,35,60,142} They also use a flow cell/chamber to introduce the sample to the measurement range and are capable of measuring at high flow speeds (up to 50,000 cells/s).¹²⁴

Flow cytometry has proven its position as a standard high-throughput ELS measurement method. Among clinical applications of light scattering is RBC characterization, based on hematologic parameters such as mean cell volume, mean cell hemoglobin concentration, mean cell hemoglobin mass, as well as red cell volume distribution.^{143,144} ELS from a single RBC enables measuring cell volume and hemoglobin.^{140,145} Extensive research has been conducted into measuring and analyzing ELS from lymphocytes and other white blood cells¹²⁴ with flow cytometry. As a theoretical understanding of light-matter interactions and flow cytometry measurements provides a wealth of information, an exact model is necessary for the characterization of different cells. The two-layer model (coated sphere) has been found as an appropriate model to describe

scattering from lymphocytes, and it can be used to solve inverse light-scattering problems.¹²⁴ Earlier work with flow cytometry has shown that, by monitoring orthogonal light scattering, it is possible to distinguish cytotoxic lymphocytes from normal ones.¹⁴⁶ An extension of normal flow cytometry, known as scanning flow cytometry,⁶⁰ enables characterizing different types of white blood cells such as T lymphocytes, neutrophils, granulocytes, and monocytes.¹²⁴ Using advanced optical models of white blood cells (coated sphere or multilayered sphere) and solving the inverse light-scattering problem allow us to differentiate between different classes of white blood cells.¹²⁴

Recently, Konokhova et al.¹⁴⁷ demonstrated the use of the scanning flow cytometer to measure angle-resolved light-scattering patterns of individual blood microparticles. By fitting experimental curves with the homogeneous sphere model, they were able to determine the size and refractive index of particles, thus demonstrating the possibility of label-free identification of blood microparticles, i.e., their separation from the nonspherical constituents of platelet-rich plasma. This submicron size range is an important and topical research area that requires new characterization methods.

A new method has recently been developed to measure 2-D light-scattering images from single cells in a flow cytometry instrument. It takes advantage of 2-D imaging sensors to record the angular distribution of coherently scattered light from flowing particles and cells.^{148–150} This method is being developed to facilitate label-free cell classification and extraction of 3-D morphological features.¹⁵⁰ Neukammer et al. used two wavelengths to separate different blood cells. They used an optical trap to position and orient single particles and particle clusters to investigate differential light scattering and demonstrated the analysis of optically trapped microspheres with light scattering from a 2-D image.¹⁴⁹

4 Applications and Future Perspective

Multimodal instruments allow the simultaneous application of complementary methods of studying an object. Smith and Berger¹⁵¹ developed an instrument that enables measuring ELS in combination with Raman signals to characterize different cells, lymphocytes, and granulocytes. This permits measuring the morphology and chemistry of cells without labeling

them with, for example, fluorescence dyes. It is worth noting that when using a tightly focused laser beam for illumination, Mie theory needs to be extended to account for the non-negligible cone angle of the Gaussian beam.¹⁵¹

Refractive index matching (optical clearing) forms the basis for developing methods to modify optical properties, to improve light penetration, and to reduce scattering.^{152–154} Optical clearing has been studied at the cellular level in different contexts. Mourant et al.⁹⁴ studied light scattering from cell suspensions. Due to the different refractive indices of cell and tissue components as well as PBS, the scattering properties of cells can be modeled using different background suspensions with various refractive indices. Mourant and her team found that the scattering from particles in contact with the medium decreased when the medium's refractive index increased. This mimics the situation when cells are close to each other, as in a tissue.

Popescu et al.¹⁵⁵ monitored single RBCs during hemolysis with Hilbert phase microscopy. They established that as hemoglobin flushes out, refractive indices will be matched. In both research papers described above,^{94,155} the key physical principle involved matching the refractive indices of the cell surface and the background medium, thereby changing the optical properties of the cell (μ_s , g). Local hemolysis has also been studied theoretically.¹⁵⁶

We recently studied the effect of optical clearing (matching of refractive indices) at the single-cell and single-particle levels.^{110,157} Optical clearing strives to manipulate optical properties such that light can penetrate deeper into tissue. It relies on refractive index matching, which increases g and decreases scattering. Optical clearing also affects the scattering cross-section of cells. When an RBC was fixed in a trap and 5% glucose was used as clearing agent, the g -value increased from 0.877 to 0.944.¹¹⁰ In this line of research, the following issues are highly important and must be taken into account. If only part of the ELS signal is measured, it will lead to problems in fitting the theoretical curve and estimating the value of g . In addition, optical clearing with a high concentration of clearing solution (glycerol and glucose) changes trapping efficiency and the dynamical behavior of a cell in a trap, which needs to be considered.¹¹⁰

Current progress in wide areas of nanotechnology has made nanotoxicity an important issue. Flow cytometry and ELS have been used to characterize the cellular intake of nanoparticles.¹⁵⁸ Despite their hazardous potential, nanoparticles have a range of applications in therapy and image contrast enhancement.¹⁵⁹ There is thus an increasing need to quantify and analyze the amount of nanoparticles within cells.

Fast development of measurement methods and analysis has opened a new horizon for nonlabeled imaging and quantification of the chemical structure of single cells.^{132,160,161} Further, the implementation of separate optical elements into mobile phones enables microscopic imaging of RBCs in the field outside of research laboratories.¹⁶² Microscopic images enable measuring cell size, cell size distribution, and cell number, making ELS-based diagnostics feasible for biomedical applications.^{163–166}

5 Conclusion

This paper has reviewed a collection of theoretical and experimental papers related to ELS at the single-cell level. ELS complements other optical techniques and, being label-free, it deserves a place in this fast developing area. A combination of high experimental sensitivity and theoretical understanding is the key to future applications. Moreover, the development of

light sources enables multispectral measurements and manipulation at the single-cell and particle level. Optical tweezers have proven a powerful tool for manipulating cell orientation and enabling measurement of ELS from trapped cells. Moreover, microscopic methods and FTLs have opened new possibilities for cellular level diagnostics, particularly as new, portable ELS-based diagnostics methods are finding their way into practical use.

Acknowledgments

The authors wish to extend their thanks to the Finnish Funding Agency for Innovation (Fidipro project 40111/11) and to the Academy of Finland (277748) for financial support. They also wish to acknowledge the value of personal discussions with Prof. Valery Tuchin and Dr. Zuomin Zhao.

References

1. W. Drexler and J. G. Fujimoto, Eds., *Optical Coherence Tomography Technology and Applications, Biological and Medical Physics, Biomedical Engineering*, p 1346, Springer, Berlin, New York (2008).
2. R. Bernardes and J. Cunha-Vaz, *Optical Coherence Tomography. A Clinical and Technical Update, Biological and Medical Physics, Biomedical Engineering XV*, p 255, Springer, Berlin, Heidelberg (2012).
3. R. Wessels et al., "Optical biopsy of epithelial cancers by optical coherence tomography (OCT)," *Lasers Med. Sci.* **29**, 1297–1305 (2014).
4. Z. A. Nima et al., "Applications of surface-enhanced Raman scattering in advanced bio-medical technologies and diagnostics," *Drug Metab. Rev.* **46**(2), 155–175 (2014).
5. S. Schlucker, "Surface-enhanced Raman spectroscopy: concepts and chemical applications," *Angew. Chem. Int. Ed.* **53**, 4756–4795 (2014).
6. Y. Yanase et al., "Application of SPR imaging sensor for detection of individual living cell reactions and clinical diagnosis of type I allergy," *Allergol. Int.* **62**, 163–169 (2013).
7. C. T. Campbell and G. Kim, "SPR microscopy and its applications to high-throughput analyses of biomolecular binding events and their kinetics," *Biomaterials* **28**, 2380–2392 (2007).
8. Y. Yanase et al., "Surface plasmon resonance for cell-based clinical diagnosis," *Sensors* **14**, 4948–4959 (2014).
9. H. Tu and S. A. Boppart, "Coherent anti-Stokes Raman scattering microscopy: overcoming technical barriers for clinical translation," *J. Biophotonics* **7**(1–2), 9–22 (2014).
10. Tuan Vo-Dinh, Ed., *Biomedical Photonics Handbook*, CRC Press, Boca Raton, London, New York, Washington, DC (2003).
11. P. C. Waterman, "Matrix formulation of electro-magnetic scattering," *Proc. IEEE* **53**, 805 (1965).
12. P. C. Waterman, "Symmetry, unitarity, and geometry in electro-magnetic scattering," *Phys. Rev. D* **3**, 825 (1971).
13. S. K. Yee, "Numerical solution of initial boundary value problems involving Maxwell's equations in isotropic media," *IEEE Trans. Antennas Propag.* **14**, 302 (1966).
14. M. Mishchenko, J. Hovenier, and L. Travis, Eds., *Light Scattering by Nonspherical Particles*, Elsevier (Academic Press), London (1999).
15. T. Wriedt, "Light scattering theory and programs: discussion of latest advances and open problems," *J. Quant. Spectrosc. Radiat. Transfer* **113**(18), 2465–2469 (2012).
16. T. Wriedt, "Light scattering theory and programs: open problems and questions," *AAPP Phys. Math. Nat. Sci.* **89**(Suppl. No.1), C1V89S1P014 (5pages) (2011).
17. M. I. Mishchenko et al., "Comprehensive T-matrix reference database: a 2011–2013 update," *J. Quant. Spectrosc. Radiat. Transfer* **123**, 145–152 (2013).
18. M. I. Mishchenko et al., "Comprehensive T-matrix reference database: a 2013–2014 update," *J. Quant. Spectrosc. Radiat. Transfer* **146**, 349–354 (2014).
19. M. Kerker and M. I. Hampton, "The use of unfiltered light in determining particle radius by the polarization ratio of scattered light," *J. Opt. Soc. Am.* **43**(5), 370–371 (1953).

20. D. L. Jaggard et al., "Light scattering from particles of regular and irregular shape," *Atmos. Environ.* **15**(12), 2511–2519 (1981).
21. O. Munoz and J. W. Hovenier, "Laboratory measurements of single light scattering by ensembles of randomly oriented small irregular particles in air. A review," *J. Quant. Spectrosc. Radiat. Transfer* **112**, 1646–1657 (2011).
22. P. J. Wyatt, "Differential light scattering: a physical method for identifying living bacterial cells," *Appl. Opt.* **7**, 1879 (1968).
23. A. Brunsting and P. F. Mullaney, "Light scattering from coated spheres: model for biological cells," *Appl. Opt.* **11**(3), 675–680 (1972).
24. A. Dunn and R. Richards-Kortum, "Three-dimensional computation of light scattering from cells," *Sel. Top. Quantum Electron.* **2**(4), 898–905 (1996).
25. P. F. Mullaney et al., "Cell sizing: a light scattering photometer for rapid volume determination," *Rev. Sci. Instrum.* **40**, 1029–1032 (1969).
26. M. Kerker et al., "Light scattering and fluorescence by small particles having internal structure," *J. Histochem. Cytochem.* **27**, 250–263 (1979).
27. M. Kerker, "Elastic and in elastic light scattering in flow cytometry (Paul Mullaney Memorial Lecture)," *Cytometry* **4**, 1–10 (1983).
28. J. R. Mourant et al., "Mechanisms of light scattering from biological cells relevant to noninvasive optical-tissue diagnostics," *Appl. Opt.* **37**(16), 3586–3593 (1998).
29. A. Alberts et al., *Molecular Biology of the Cell*, pp. 18–19, Garland, New York (1994).
30. G. C. Salzman et al., "Cell classification by laser light scattering: identification and separation of unstained leukocytes," *Acta Cytol.* **19**, 374–377 (1975).
31. M. R. Loken, R. G. Sweet, and L. A. Herzenberg, "Cell discrimination by multiangle light scattering," *J. Histochem. Cytochem.* **24**, 284–291 (1976).
32. M. Bartholdi et al., "Differential light scattering photometer for rapid analysis of single particles in flow," *Appl. Opt.* **19**, 1573–1581 (1980).
33. R. M. P. Doornbos et al., "Elastic light-scattering measurements of single biological cells in an optical trap," *Appl. Opt.* **35**, 729–734 (1996).
34. K. A. Sem'yanov et al., "Calibration-free method to determine the size and hemoglobin concentration of individual red blood cells from light scattering," *Appl. Opt.* **39**(31), 5884–5889 (2000).
35. M. A. Yurkin et al., "Experimental and theoretical study of light scattering by individual mature red blood cells by use of scanning flow cytometry and a discrete dipole approximation," *Appl. Opt.* **44**(25), 5249–5256 (2005).
36. N. N. Boustany and N. V. Thakor, "Light scatter spectroscopy and imaging of cellular and subcellular events," Chapter 16 in *Biomedical Photonics Handbook*, Tuan Vo-Dinh, Ed., CRC Press, Boca Raton, London, New York, Washington, DC (2003).
37. T. T. Wu and J. Y. Qu, "Assessment of the relative contribution of cellular components to the acetowhitening effect in cell cultures and suspensions using elastic light-scattering spectroscopy," *Appl. Opt.* **46**(21), 4834–4842 (2007).
38. V. V. Tuchin, *Tissue Optics: Light Scattering Methods and Instruments for Medical Diagnosis*, 2nd ed., PM 166, p. 840, SPIE Press, Bellingham, Washington (2007).
39. N. N. Boustany, S. A. Boppart, and V. Backman, "Microscopic imaging and spectroscopy with scattered light," *Annu. Rev. Biomed. Eng.* **12**, 285–314 (2010).
40. H. Fang et al., "Noninvasive sizing of subcellular organelles with light scattering spectroscopy," *Sel. Top. Quantum Electron.* **9**(2), 267–276 (2003).
41. C. S. Mulvey et al., "Wavelength-dependent backscattering measurements for quantitative monitoring of apoptosis, Part 2: early spectral changes during apoptosis are linked to apoptotic volume decrease," *J. Biomed. Opt.* **16**(11), 117002 (2011).
42. V. V. Tuchin, Ed., *Handbook of Optical Biomedical Diagnostics*, SPIE Press, Bellingham, Washington (2002).
43. L. Rayleigh, "On the light from the sky, its polarization and colour," *Philos. Mag.* **XLI**, 107–120, 274–279 (1871).
44. L. Rayleigh, "On the scattering of light by small particles," *Philos. Mag.* **XLI**, 447–454 (1871).
45. L. Rayleigh, "On the transmission of light through an atmosphere containing small particles in suspension, and on the origin of the blue of the sky," *Philos. Mag.* **XLVII**, 375–384 (1899).
46. G. Mie, "Beiträge zur Optik trüber Medien, speziell kolloidaler Metallösungen," *Ann. Phys.* **330**(3), 377–445 (1908).
47. G. Mie, "Contributions to the optics of turbid media, particularly of colloidal metal solutions," *R. Aircr. Establ., Libr. Transl.* **1873**, 1–72 (1976).
48. A. E. H. Love, "The scattering of electric waves by a dielectric sphere," *Proc. London Math. Soc.* **30**(678), 308–321 (1899).
49. C. F. Bohren and D. R. Huffman, *Absorption and Scattering of Light by Small Particles*, Wiley, New York (1983).
50. H. C. van de Hulst, *Light Scattering by Small Particles*, John Wiley & Sons Inc., New York (1957); also Dover Publications Inc., New York (1981).
51. R. G. Newton, *Scattering Theory of Waves and Particles*, 2nd ed., Springer-Verlag, New York (1982, 2002).
52. T. Wriedt, "A review of elastic light scattering theories," *Part. Part. Syst. Charact.* **15**, 67–74 (1998).
53. N. A. Logan, "Early history of the Mie solution," *J. Opt. Soc. Am.* **52**, 342 (1962).
54. N. A. Logan, "Survey of some early studies of the scattering of plane waves by a sphere," *Proc. IEEE* **53**(8), 773–785 (1965).
55. A. L. Aden and M. Kerker, "Scattering of electromagnetic waves from two concentric spheres," *J. Appl. Phys.* **22**, 1242 (1951).
56. M. I. Mishchenko, L. D. Travis, and A. A. Lacis, *Scattering, Absorption, and Emission of Light by Small Particles*, Cambridge University Press, Cambridge (2002).
57. M. G. Macey, Ed., *Flow Cytometry: Principles and Applications*, Humana Press, Totowa, New Jersey (2007).
58. S. Papandreou, Ed., *Flow Cytometry: Principles, Methodology and Applications (Cell Biology Research Progress)*, Nova Science Publishers, New York (2013).
59. V. V. Tuchin, Ed., *Advanced Optical Flow Cytometry: Methods and Disease Diagnoses*, Wiley-VCH, Weinheim (2011).
60. Scanning Flow Cytometry, Cytometry and Biokinetics Laboratory Institute of Chemical Kinetics and Combustion, Novosibirsk, Russia, <http://www.kinetics.nsc.ru/lipc/cyto/sfc01.html> (27 February 2015).
61. L. T. Perelman and V. Backman, "Light scattering spectroscopy of epithelial tissues: principles and applications," Chapter 12 in *Handbook of Optical Biomedical Diagnostics*, SPIE Press, Bellingham, Washington (2002).
62. D. Y. Orlova et al., "Light scattering by neutrophils: model, simulation, and experiment," *J. Biomed. Opt.* **13**, 054057 (2008).
63. J. R. Mourant et al., "Polarized angular dependent spectroscopy of epithelial cells and epithelial cell nuclei to determine the size scale of scattering structures," *J. Biomed. Opt.* **7**(3), 378–387 (2002).
64. J. R. Mourant et al., "Angular dependent light scattering from multicellular spheroids," *J. Biomed. Opt.* **7**(1), 93–99 (2002).
65. V. V. Tuchin, L. Wang, and D. A. Zimnyakov, *Optical Polarization in Biomedical Applications*, Springer-Verlag, Berlin, Heidelberg (2006).
66. H. Ding et al., "Angle-resolved Mueller matrix study of light scattering by B-cells at three wavelengths of 442, 633, and 850 nm," *J. Biomed. Opt.* **12**(3), 034032 (2007).
67. S. Bartel and A. H. Hielscher, "Monte Carlo simulations of the diffuse backscattering Mueller matrix for highly scattering media," *Appl. Opt.* **39**(10), 1580–1588 (2000).
68. E. Eremina, Y. Eremin, and T. Wriedt, "Analysis of light scattering by erythrocyte based on discrete sources method," *Opt. Commun.* **244**, 15–23 (2005).
69. E. Eremina et al., "Different shape models for erythrocyte: light scattering analysis based on the discrete sources method," *J. Quant. Spectrosc. Radiat. Transfer* **102**, 3–10 (2006).
70. D. Petrov, Y. Shkuratov, and G. Videen, "Light scattering by arbitrary shaped particles with rough surfaces: Sh-matrices approach," *J. Quant. Spectrosc. Radiat. Transfer* **113**, 2406–2418 (2012).
71. L. Nagdimunov, L. Kolokolova, and D. Mackowski, "Characterization and remote sensing of biological particles using circular polarization," *J. Quant. Spectrosc. Radiat. Transfer* **131**, 59–65 (2013).
72. L. Bi and P. Yang, "Modeling of light scattering by biconcave and deformed red blood cells with the invariant imbedding T-matrix method," *J. Biomed. Opt.* **18**(5), 055001 (2013).
73. M. I. Mishchenko, L. D. Travis, and D. W. Mackowski, "T-matrix computations of light scattering by nonspherical particles: a review," *J. Quant. Spectrosc. Radiat. Transfer* **55**(5), 535–575 (1996).

74. M. Canpolat and J. R. Mourant, "Particle size analysis of turbid media with a single optical fiber in contact with the medium to deliver and detect white light," *Appl. Opt.* **40**(22), 3792–3799 (2001).
75. V. V. Tuchin and G. B. Altshuler, "Dental and oral tissue optics," Chapter 9, in *Fundamentals and Applications of Biophotonics in Dentistry, Vol. 4 Series on Biomaterials and Bioengineering*, p 327, A. Kishen and A. Asundi, Eds., Imperial College Press, London (2007).
76. R. Graaff et al., "Reduced light scattering properties for mixtures of spherical particles: a simple approximation derived from Mie calculations," *Appl. Opt.* **31**(10), 1370–1376 (1992).
77. S. L. Jacques, "Optical properties of biological tissues: a review," *Phys. Med. Biol.* **58**, R37–R61 (2013).
78. J. R. Mourant et al., "Influence of the scattering phase function on light transport measurements in turbid media performed with small source-detector separations," *Opt. Lett.* **21**(7), 546–548 (1996).
79. "Light Scattering Information Portal for the light scattering community," <http://www.scattport.org/> (27 February 2015).
80. Guangran Kevin Zhu, "Matlab Central: Sphere scattering," <http://www.mathworks.com/matlabcentral/fileexchange/31119-sphere-scattering> (27 February 2015).
81. Mirosław Jonasz, "MJC Optical Technology: Light scattering calculation: coated sphere," <http://www.mjcopticaltech.com/Products/LscCoatSphHelp.htm#Introduction> (27 February 2015).
82. O. Pena-Rodriguez, P. P. G. Perez, and U. Pal, "MieLab: a software tool to perform calculations on the scattering of electromagnetic waves by multilayered spheres," *Int. J. Spectrosc.* **2011**, 583743 (2011).
83. Scott Prahl, "Oregon Medical Laser Center; Mie Scattering," <http://omlc.org/software/mie/> (27 February 2015).
84. Bernhard Michel, "MieCalc—freely configurable program for light scattering calculations (Mie theory)," <http://www.lightscattering.de/MieCalc/index.html> (27 February 2015).
85. J. Hellmers and T. Wriedt, "Classification of software for the simulation of light scattering and realization within an internet information portal," *J. Univers. Comput. Sci.* **16**(9), 1176–1189 (2010).
86. J. Hellmers et al., "ScattPort light scattering internet information portal: present state and further development," in *Electromagnetic and Light Scattering XII*, K. Muinonen, A. Penttilä, and H. Lindqvist, Eds., pp. 74–77, University of Helsinki, Helsinki (2010).
87. Laven Philip, "MiePlot: A computer program for scattering of light from a sphere using Mie theory & the Debye series," <http://www.philiplaven.com/mieplot.htm> (27 February 2015).
88. J. Hellmers et al., "Customizable web service interface for light scattering simulation programs," *J. Quant. Spectrosc. Radiat. Transfer* **113**, 2243–2250 (2012).
89. J. Leinonen, "High-level interface to T-matrix scattering calculations: architecture, capabilities and limitations," *Opt. Express* **22**(2), 1655–1660 (2014).
90. M. A. Yurkin and A. G. Hoekstra, "The discrete-dipole-approximation code ADDA: capabilities and known limitations," *J. Quant. Spectrosc. Radiat. Transfer* **112**, 2234–2247 (2011).
91. M. Hammer et al., "Single scattering by red blood cells," *Appl. Opt.* **37**(31), 7410–7418 (1998).
92. J. M. Steinke and A. P. Shepherd, "Comparison of Mie theory and the light scattering of red blood cells," *Appl. Opt.* **27**(19), 4027–4033 (1988).
93. R. Drezek, A. Dunn, and R. Richards-Kortum, "Light scattering from cells: finite-difference time-domain simulations and goniometric measurements," *Appl. Opt.* **38**(16), 3651–3661 (1999).
94. J. R. Mourant et al., "Light scattering from cells: the contribution of the nucleus and the effects of proliferative status," *J. Biomed. Opt.* **5**(2), 131–137 (2000).
95. D. Watson et al., "Elastic light scattering from single cells: orientational dynamics in optical trap," *Biophys. J.* **87**(2), 1298–1306 (2004).
96. H. Ding et al., "Fourier transform light scattering of biological structure and dynamics," *IEEE J. Sel. Top. Quantum Electron.* **16**(4), 909–918 (2010).
97. J. R. Mourant, T. M. Johnson, and J. P. Freyer, "Characterizing mammalian cells and cell phantoms by polarized backscattering fiber-optic measurements," *Appl. Opt.* **40**(28), 5114–5123 (2001).
98. C. S. Mulvey, I. J. Bigio, and C. A. Sherwood, "Wavelength-dependent backscattering measurements for quantitative real-time monitoring of apoptosis in living cells," *J. Biomed. Opt.* **14**(6), 064013 (2009).
99. A. Amelink and H. J. C. M. Sterenberg, "Measurement of the local optical properties of turbid media by differential path-length spectroscopy," *Appl. Opt.* **43**(15), 3048–3054 (2004).
100. M. Kinnunen et al., "Effect of the size and shape of a red blood cell on elastic light scattering properties at the single-cell level," *Biomed. Opt. Express* **2**, 1803–1814 (2011).
101. M. Kinnunen et al., "Low-intensity light detection methods for selected biophotonic applications," *Proc. SPIE* **9421**, 94210D (2014).
102. R. A. Bolt and F. F. M. de Mul, "Goniometric instrument for light scattering measurement of biological tissues and phantoms," *Rev. Sci. Instrum.* **73**(5), 2211–2213 (2002).
103. F. Foschum and A. Kienle, "Optimized goniometer for determination of the scattering phase function of suspended particles: simulations and measurements," *J. Biomed. Opt.* **18**(8), 085002 (2013).
104. R. Ceolato et al., "Light-scattering by aggregates of tumor cells: spectral, polarimetric, and angular measurements," *J. Quant. Spectrosc. Radiat. Transfer* **146**, 207–213 (2014).
105. A. Brunsting and P. F. Mullaney, "Differential light scattering from spherical mammalian cells," *Biophys. J.* **14**, 439–453 (1974).
106. M. R. Arnfield, J. Tulip, and M. S. McPhee, "Optical propagation in tissue with anisotropic scattering," *IEEE Trans. Biomed. Eng.* **35**(5), 372–381 (1988).
107. J. D. Wilson et al., "Light scattering from intact cells reports oxidative-stress-induced mitochondrial swelling," *Biophys. J.* **88**, 2929–2938 (2005).
108. H. Holthoff et al., "Coagulation rate measurement of colloidal particles by simultaneous static and dynamic light scattering," *Langmuir* **12**, 5541–5549 (1996).
109. A. Kauppila et al., "Elastic light scattering measurements from multiple red blood cells in elliptical optical tweezers," *Proc. SPIE* **8097**, 80970K (2011).
110. M. Kinnunen et al., "Optical clearing at a cellular level," *J. Biomed. Opt.* **19**(7), 071409 (2014).
111. M. Kinnunen et al., "Measurement of elastic light scattering from two optically trapped microspheres and red blood cells in a transparent medium," *Opt. Lett.* **36**(18), 3554–3556 (2011).
112. P. J. Wyatt, "Light scattering and the absolute characterization of macromolecules," *Anal. Chim. Acta* **272**, 1–40 (1993).
113. W. Kaller, "A new polar nephelometer for measurement of atmospheric aerosols," *J. Quant. Spectrosc. Radiat. Transfer* **87**, 107–117 (2004).
114. J.-L. Castagner and I. J. Bigio, "Polar nephelometer based on rotational confocal imaging setup," *Appl. Opt.* **45**(10), 2232–2239 (2006).
115. J.-L. Castagner and I. J. Bigio, "Particle sizing with a fast polar nephelometer," *Appl. Opt.* **46**(4), 527–532 (2007).
116. A. Ashkin et al., "Observation of a single-beam gradient force optical trap for dielectric particles," *Opt. Lett.* **11**, 288–290 (1986).
117. W. H. Wright et al., "Measurement of light scattering from cells using an inverted infrared optical trap," *Proc. SPIE* **1427**, 279–287 (1991).
118. P. Li, K. Shi, and Z. Liu, "Manipulation and spectroscopy of a single particle by use of white-light optical tweezers," *Opt. Lett.* **30**(2), 156–158 (2005).
119. P. Li, K. Shi, and Z. Liu, "Optical scattering spectroscopy by using tightly focused supercontinuum," *Opt. Express* **13**(22), 9039–9044 (2005).
120. M. Guillon, K. Dholakia, and D. McGloin, "Optical trapping and spectral analysis of aerosols with a supercontinuum laser source," *Opt. Express* **16**(11), 7655–7664 (2008).
121. J. D. Wilson and T. H. Foster, "Mie theory interpretations of light scattering from intact cells," *Opt. Lett.* **30**(18), 2442–2444 (2005).
122. J. D. Wilson, "Measurements and interpretations of light scattering from intact biological cells," Thesis: Doctor of Philosophy, pp 231, University of Rochester, New York (2007).
123. Y. R. Kim and L. Ornstein, "Isovolumetric sphering of erythrocytes for more accurate and precise cell volume measurement by flow cytometry," *Cytometry* **3**(6), 419–427 (1983).
124. V. P. Maltsev, A. G. Hoekstra, and M. A. Yurkin, "Optics of white blood cells: optical models, simulations, and experiments," in *Advanced Optical Flow Cytometry: Methods and Disease Diagnoses*, V. V. Tuchin, Ed., Wiley-VCH, Weinheim (2011).
125. S. V. Tsinopoulos and D. Polyzos, "Scattering of He-Ne laser light by an average-sized red blood cell," *Appl. Opt.* **38**, 5499–5510 (1999).
126. A. Karlsson et al., "Numerical simulations of light scattering by red blood cells," *IEEE Trans. Biomed. Eng.* **52**, 13–18 (2005).

127. A. M. K. Nilsson et al., "T-matrix computations of light scattering by red blood cells," *Appl. Opt.* **37**, 2735–2748 (1998).
128. J. He et al., "Light scattering by multiple red blood cells," *J. Opt. Soc. Am. A* **21**, 1953–1961 (2004).
129. T. Wriedt et al., "Light scattering by single erythrocyte: comparison of different methods," *J. Quant. Spectrosc. Radiat. Transfer* **100**, 444–456 (2006).
130. H. Ding et al., "Fourier transform light scattering of inhomogeneous and dynamic structures," *Phys. Rev. Lett.* **101**, 238102 (2008).
131. Y. Park et al., "Static and dynamic light scattering of healthy and malaria-parasite invaded red blood cells," *J. Biomed. Opt.* **15**(2), 020506 (2010).
132. Y. Park et al., "Spectroscopic phase microscopy for quantifying hemoglobin concentrations in intact red blood cells," *Opt. Lett.* **34**(23), 3668–3670 (2009).
133. J. Lim et al., "Born approximation model for light scattering by red blood cells," *Biomed. Opt. Express* **2**(10), 2784–2791 (2011).
134. Y. Kim et al., "Anisotropic light scattering of individual sickle red blood cells," *J. Biomed. Opt.* **17**(4), 040501 (2012).
135. Y. Jo et al., "Angle-resolved light scattering of individual rod-shaped bacteria based on Fourier transform light scattering," *Sci. Rep.* **4**, 5090 (2014).
136. J. Jung and Y. Park, "Spectro-angular light scattering measurements of individual microscopic objects," *Opt. Express* **22** (4), 4108–4114 (2014).
137. R. S. Brock et al., "Effect of detailed cell structure on light scattering distribution: FDTD study of a B-cell with 3D structure constructed from confocal images," *J. Quant. Spectrosc. Radiat. Transfer* **102**, 25–36 (2006).
138. I. Itzkan et al., "Confocal light absorption and scattering spectroscopic microscopy monitors organelles in live cells with no exogenous labels," *Proc. Natl. Acad. Sci. U. S. A.* **104**(44), 17255–17260 (2007).
139. V. Richter et al., "Light scattering microscopy with angular resolution and its possible application to apoptosis," *J. Microsc.* **257**(1), 1–7 (2015).
140. D. H. Tycko et al., "Flow-cytometric light scattering measurement of red blood cell volume and hemoglobin concentration," *Appl. Opt.* **24**(9), 1355–1365 (1985).
141. M. Brown and C. Wittwer, "Flow cytometry: principles and clinical applications in hematology," *Clin. Chem.* **46**(8), 1221–1229 (2000).
142. V. P. Maltsev, "Scanning flow cytometry for individual particle analysis," *Rev. Sci. Instrum.* **71**(1), 243–255 (2000).
143. M. M. Wintrobe et al., *Clinical Hematology*, p. 18, Lea & Febiger, Philadelphia, Pennsylvania (1981).
144. J. D. Bessman and R. K. Johnson, "Erythrocyte volume distribution in normal and abnormal subjects," *Blood* **46**, 369 (1975).
145. N. Mohandas et al., "Accurate and independent measurement of volume and hemoglobin concentration of individual red cells by laser light scattering," *Blood* **68**(2), 506–513 (1986).
146. L. W. Terstappen et al., "Discrimination of human cytotoxic lymphocytes from regulatory and B-lymphocytes by orthogonal light scattering," *J. Immunol. Methods* **95**, 211–216 (1986).
147. A. I. Konokhova et al., "Light-scattering flow cytometry for identification and characterization of blood microparticles," *J. Biomed. Opt.* **17**(5), 057006 (2012).
148. S. Holler et al., "Two-dimensional angular optical scattering for the characterization of airborne microparticles," *Opt. Lett.* **23**, 1489–1491 (1998).
149. J. Neukammer et al., "Angular distribution of light scattered by single biological cells and oriented particle agglomerates," *Appl. Opt.* **42**(31), 6388–6397 (2003).
150. X.-H. Hu and J. Q. Lu, "Label-free cell classification with diffraction imaging flow cytometer," in *Advanced Optical Flow Cytometry: Methods and Disease Diagnoses*, V. V. Tuchin, Ed., Wiley-VCH, Weinheim (2011).
151. Z. J. Smith and A. J. Berger, "Validation of an integrated Raman- and angular scattering microscopy system on heterogeneous bead mixtures and single human immune cells," *Appl. Opt.* **48**(10), D109–D120 (2009).
152. E. A. Genina, A. N. Bashkatov, and V. V. Tuchin, "Tissue optical immersion clearing," *Expert Rev. Med. Devices* **7**(6), 825–842 (2010).
153. V. V. Tuchin, *Optical Clearing of Tissues and Blood*, p. 256, SPIE Press, Bellingham, Washington (2006).
154. D. Zhu et al., "Recent progress in tissue optical clearing," *Laser Photonics Rev.* **7**(5), 732–757 (2013).
155. G. Popescu et al., "Erythrocyte structure and dynamics quantified by Hilbert phase microscopy," *J. Biomed. Opt.* **10**(6), 060503 (2005).
156. V. V. Tuchin et al., "Theoretical study of immersion optical clearing of blood in vessels at local hemolysis," *Opt. Express* **12**, 2966–2971 (2004).
157. M. Kinnunen et al., "Optical tweezers-assisted measurements of elastic light scattering," *Proc. SPIE* **9031**, 90310A (2014).
158. H. Suzuki, T. Toyooka, and Y. Ibuki, "Simple and easy method to evaluate uptake potential of nanoparticles in mammalian cells using a flow cytometric light scatter analysis," *Environ. Sci. Technol.* **41**, 3018–3024 (2007).
159. L. Dykman and N. Khlebtsov, "Gold nanoparticles in biomedical applications: recent advances and perspectives," *Chem. Soc. Rev.* **41**(6), 2256–2282 (2012).
160. K. Kim et al., "High-resolution three-dimensional imaging of red blood cells parasitized by Plasmodium falciparum and *in situ* hemozoin crystals using optical diffraction tomography," *J. Biomed. Opt.* **19**(1), 011005 (2014).
161. T. Kim et al., "White-light diffraction tomography of unlabelled live cells," *Nat. Photonics* **8**, 256–263 (2014).
162. A. Skandarajah et al., "Quantitative imaging with a mobile phone microscope," *PLoS One* **9**(5), e96906 (2014).
163. Z. J. Smith, K. Chu, and S. Wachsmann-Hogiu, "Nanometer-scale sizing accuracy of particle suspensions on an unmodified cell phone using elastic light scattering," *PLoS One* **7**(10), e46030 (2012).
164. Z. J. Smith et al., "Cell-phone-based platform for biomedical device development and education applications," *PLoS One* **6**(3), e17150 (2011).
165. Q. Wei et al., "Detection and spatial mapping of mercury contamination in water samples using a smart-phone," *ACS Nano* **8**(2), 1121–1129 (2014).
166. H. Zhu et al., "Cost-effective and rapid blood analysis on a cell-phone," *Lab Chip* **13**(7), 1282–1288 (2013).

Matti Kinnunen received his MSc (Tech) and DSc (Tech.) degrees in electrical engineering from the University of Oulu, Oulu, Finland, in 2002 and 2006, respectively. He is currently working as a senior research fellow at the University of Oulu. His research interests include light-matter interactions in tissues and at the single-cell level, sensors, and measurement techniques, as well as optical noninvasive measurement techniques for biomedical applications.

Artashes Karmenyan has his PhD degree in physics-mathematics from Yerevan State University (YSU), Armenia. He was head of the Spectroscopy Laboratory in "Laseraim Technika" Institute, YSU, then joined the Laboratory of Laser Methods for Tumor Diagnosis and Therapy, Cancer Research Center, Moscow, Russia. Since 2001 he has worked in Taiwan, in National Yang-Ming University and National Dong-Hwa University, in the fields of laser spectroscopy (Raman, fluorescence, time-resolved), biomedical applications, and noninvasive optical techniques for mammalian embryos research and reconstruction.